SCIENCE CHINA
Information Sciences

• **RESEARCH PAPERS** •

December 2010 Vol. 53 No. 12: 2653–2663
doi: 10.1007/s11432-010-4117-3

Improved innovation-based adaptive Kalman filter for dual-frequency navigation using carrier phase

LU ChenXi, TAN YunHua*, ZHU BoCheng & ZHOU LeZhu

School of Electronics Engineering and Computer Science, Peking University, Beijing 100871*, China*

Received July 24, 2010; accepted September 13, 2010

Abstract A new adaptive Kalman filtering algorithm for dual-frequency navigation using carrier phase is presented. This algorithm gives consideration to both robustness and sensitivity by combining the two main approaches of adaptive Kalman filtering based on innovation-based adaptive estimation (IAE) and fading filtering. Applicable to the navigation using carrier phase measurements typically, this algorithm can balance the weights of observations and predicted states preferably. Applications to both practical static data and kinetic simulations are presented to demonstrate the validity and efficiency of the algorithm.

Keywords navigation, adaptive Kalman filter, carrier phase

Citation Lu C X, Tan Y H, Zhu B C, et al. Improved innovation-based adaptive Kalman filter for dual-frequency navigation using carrier phase. Sci China Inf Sci, 2010, 53: 2653–2663, doi: 10.1007/s11432-010-4117-3

1 Introduction

Robustness and precision are of the most important considerations in navigation algorithm, especially in kinetic cases. Because of the inconsistency of the two considerations mentioned, adaptive Kalman filters are widely used to improve the quality of navigation in various environments [1–5]. Compared to the classic Kalman filter, adaptive Kalman filter can adjust covariance matrix of observations and predicted states adaptively when the receiver's motion parameters or observations' noise intensity changes. Various approaches of adaptive Kalman filtering have been proposed [3–7], among which there are mainly two effective methods for navigation, named innovation-based adaptive estimation (IAE) [3, 6] and fading filtering [2]. Conventional IAE method assumes the state covariance steadies and updates Kalman gain by estimating the covariance of observations every epoch. An improved IAE method estimates the state covariance at the same time which is also named Residual-based adaptive estimation (RAE) [6], because the covariance is estimated based on observation residual. Disadvantageously, in IAE or RAE method, the covariance is estimated in a moving window and the width of the window must be known. Besides, changes of the kinetic state or observations' distribution in the window may lower the precision of estimation. Another kind of approaches based on fading filtering uses fading factors to weaken the distribution of old information and keeps Kalman gain updating every epoch. The disadvantages of this method are that fading factors influence filtering process directly, making the inconsistency of stability

*Corresponding author (email: tanggeric@pku.edu.cn)

and sensitivity more serious, and that usually this method can only adapt narrow kinetic range because it is difficult to set proper fading factors. Therefore, an improved adaptive algorithm for Kalman filter, which combines RAE and fading filtering methods, is presented in this paper. Its ideal can also be applied to other fields such as mobile communications [8].

In the new adaptive Kalman filter, covariance matrixes of observations and states are estimated separately, and the fading factor influences filtering process indirectly by influencing the estimation. A new fading factor is also proposed to estimate the covariance matrix of observations, while the covariance matrix of states is updated based on the filtering states. Advantages of the new algorithm are that, estimating covariance matrixes every epoch keeps the filter adapting motion of the receivers more sensitively. Also, the fading factor does not influence filtering process directly but are used in the estimation to enlarge the dynamic range.

Furthermore, this new filtering algorithm is applied to navigation using carrier phase typically in this paper to prove its effectiveness. Carrier phase observations are usually used in navigation to improve precision because of their low noise intensity [9, 10]. In such cases, adaptation of the navigation algorithm is of great importance because motion of the receiver affects the filtering process more seriously. Without proper adaptation algorithm, precision of navigation cannot be guaranteed, and even worse, filtering divergence may occur.

The paper proceeds as follows: Observation model for Kalman filter using carrier phase observations is given in section 2. The new adaptive filtering algorithm is illustrated in detail in section 3. The practical application and kinetic simulation of the algorithm are presented in section 4. Section 5 gives a brief summary of the obtained results as the conclusion.

2 Establishment of the observation equation set using carrier phase

Take global positioning system (GPS) as an example. The dual-frequency code pseudorange and carrier phase observations from each satellite can be given by

$$\Phi_1^i = \frac{\rho_i}{\lambda_1} - \frac{I_i}{\lambda_1} + N_1^i + \varepsilon_{\Phi 1}^i, \tag{1a}$$

$$\Phi_2^i = \frac{\rho_i}{\lambda_2} - \frac{f_1^2}{f_2^2} \cdot \frac{I_i}{\lambda_2} + N_2^i + \varepsilon_{\Phi 2}^i, \tag{1b}$$

$$P_1^i = \rho_i + I_i + \varepsilon_{P1}^i, \tag{1c}$$

$$P_2^i = \rho_i + \frac{f_1^2}{f_2^2} I_i + \varepsilon_{P2}^i, \tag{1d}$$

where f_1, f_2 denote the two frequencies of observations, λ_1, λ_2 are the wavelengths of the two frequencies, i is the satellite identification, Φ_1^i, Φ_2^i and P_1^i, P_2^i are carrier phase and code pseudorange observations, ρ_i denotes the pseudorange free of ionospheric influence, I_i is the ionospheric delay on f_1 frequency, N_1^i and N_2^i are the ambiguities of the carrier phase observations on the two frequencies, and ε denotes the measurement error. Other error sources such as troposphere are viewed as corrected and the residuals are added on ε.

In point positioning and navigation, the two carrier phase ambiguities of each satellite may not be integers, so taking ambiguities as estimators in Kalman filter is an effective solution. Therefore, $4 + 2n$ independent unknown values are used to estimate in navigation computing when observations of n satellites are taken into the solution. Considering the ionospheric refraction correction and the number of unknowns, observation equation set can be established based on the U of C observation model [11] and eq. (1) as

$$\boldsymbol{Y}_i = \begin{bmatrix} f_{11} \cdot \lambda_1 \Phi_1^i - f_{22} \cdot \lambda_2 \Phi_2^i \\ (P_1^i + \lambda_1 \Phi_1^i)/2 \\ (P_2^i + \lambda_2 \Phi_2^i)/2 \end{bmatrix} = \begin{bmatrix} 1 & f_{11}\lambda_1 & -f_{22}\lambda_2 \\ 1 & \lambda_1/2 & 0 \\ 1 & 0 & \lambda_2/2 \end{bmatrix} \cdot \begin{bmatrix} \rho_i \\ N_1^i \\ N_2^i \end{bmatrix} + \begin{bmatrix} \varepsilon_1^i \\ \varepsilon_2^i \\ \varepsilon_3^i \end{bmatrix}, \tag{2}$$

where

$$f_{11} = \frac{f_1^2}{f_1^2 - f_2^2}, \quad f_{22} = \frac{f_2^2}{f_1^2 - f_2^2}, \tag{3a}$$

$$\varepsilon_1^i = f_{11} \cdot \lambda_1 \varepsilon_{\Phi 1}^i - f_{22} \cdot \lambda_2 \varepsilon_{\Phi 2}^i, \tag{3b}$$

$$\varepsilon_2^i = \frac{1}{2} \cdot (\lambda_1 \varepsilon_{\Phi 1}^i + \varepsilon_{P1}^i), \tag{3c}$$

$$\varepsilon_3^i = \frac{1}{2} \cdot (\lambda_2 \varepsilon_{\Phi 2}^i + \varepsilon_{P2}^i). \tag{3d}$$

By eq. (2), there are three equations of each satellite; that is, $3n$ equations are in the whole observation equation set. Considering the $4 + 2n$ independent unknown values, at least 4 satellites are needed in the solution, which equals the least requirement in classic code pseudorange solution. Therefore, the new method does not require extra chosen satellites and the satellite choosing process is the same as classic Kalman solution with code pseudoranges.

In navigation, coordinates of the receiver are direct parameters to be solved. Denote by x_s^i, y_s^i and z_s^i the coordinates of the ith satellite and by c the speed of light. Then the receiver coordinates and pseudoranges in eq. (2) can be related via

$$\rho_i = \sqrt{(x_s^i - x)^2 + (y_s^i - y)^2 + (z_s^i - z)^2} + c \cdot b, \tag{4}$$

where x, y and z are the three-dimensional coordinates of receiver in Earth-centered Earth-fixed (ECEF) coordinate system and b is the receiver's clock error. Usually, a rough position of the receiver is set to start filtering, and the one-step predicted position in Kalman filtering process is taken as the rough position every epoch. Let x_0, y_0 and z_0 be the coordinates of the rough position. Then eq. (4) can be linearized by Taylor expansion:

$$\rho_i - \rho_0^i = \left.\frac{\partial \rho_i}{\partial x}\right|_{x_0} (x - x_0) + \left.\frac{\partial \rho_i}{\partial y}\right|_{y_0} (y - y_0) + \left.\frac{\partial \rho_i}{\partial z}\right|_{z_0} (z - z_0) + c \cdot b, \tag{5a}$$

$$\rho_0^i = \sqrt{(x_s^i - x_0)^2 + (y_s^i - y_0)^2 + (z_s^i - z_0)^2}. \tag{5b}$$

Combining eqs. (2) and (5), linear observation equation set from each satellite's observations can be established separately. In order to obtain reliable results, we assemble equation sets of all chosen satellites to form the equation set for Kalman filtering. Assuming n satellites are chosen for the solution, the vector of independent unknown parameters is

$$\boldsymbol{X} = \begin{bmatrix} x & y & z & b & N_1^1 & N_2^1 & \cdots & N_1^n & N_2^n \end{bmatrix}. \tag{6}$$

In order to adapt various motion states and make estimation more precise, the state vector in Kalman filter is defined by extending eq. (6). For example, differential coefficient of the receiver clock error is usually added to the state vector because the receiver's clock usually has a significant drift. Other states such as the velocity and acceleration are also needed in the vector to adapt high dynamic range, as will be illustrated below in the adaptation of state covariance matrix.

3 Adaptive Kalman filtering algorithm

Based on the observation equation established above, we develop a new adaptive Kalman filtering algorithm to improve the stability and precision of positioning process. In the new algorithm, measurement covariance matrix is estimated based on linear combinations of phase and code observations, in which the pseudorange variable is eliminated to adapt kinetic cases. The state covariance matrix is adjusted by updating the process-noise vector based on the differences between filtering results and predicted states. We also proposed a new fading factor to balance the weights of new and old information. The new algorithm can adapt environments more widely than the fading filtering method, and at the same time is more precise and has lower calculation cost than the RAE method.

3.1 Adaptation of measurement covariance matrix

The measurement equation set for Kalman filter is established in section 2 by assembling the observation equation set form each satellites together. In practical navigation applications, the errors of direct observations are reasonably assumed to be independently distributed. Therefore, we calculate the variances of observation errors from each satellite separately to obtain the measurement covariance matrix. Because the variances of phase errors are at least two orders of magnitude less than that of code observations, they are ignored when we estimate the code error variances. After the code error variance estimation, the phase error variances are calculated roughly based on the code results. Eliminating ρ_i and I_i from eq. (1), two linear combinations of direct observations are established:

$$B_1^i = \frac{f_1\lambda_1\Phi_1^i - f_2\lambda_2\Phi_2^i}{f_1 - f_2} - \frac{f_1P_1^i + f_2P_2^i}{f_1 + f_2}, \tag{7a}$$

$$B_2^i = P_1^i - P_2^i + \lambda_1\Phi_1^i - \lambda_2\Phi_2^i, \tag{7b}$$

where B_1^i is the Melbourne-Wübbena combination usually used in cycle slip detection and B_2^i is a combination we designed for calculating the error variance on two frequencies separately. Under the independent assumption, the variances of the combinations and the observation errors are related via

$$D\{B_1^i\} = \frac{f_1^2 \cdot D\{\varepsilon_{P1}^i\} + f_2^2 \cdot D\{\varepsilon_{P2}^i\}}{(f_1 + f_2)^2}, \tag{8a}$$

$$D\{B_2^i\} = D\{\varepsilon_{P1}^i\} + D\{\varepsilon_{P2}^i\}, \tag{8b}$$

where $D\{\cdot\}$ stands for the variance of relevant variable. The phase observations are ignored as tiny quantities in eq. (8) to simplify the calculation. Cycle slips are not discussed in this paper, so the ambiguities are constant assuming cycle slips have been corrected. Therefore, the combinations in eq. (7) have constant averages and their variances are determined by the code observation errors. In practical navigation, the states of receiver are obtained by Kalman filter every epoch, so the estimation process also must be real-time. We develop a recursive method to estimate the averages and variances of the combinations every epoch, in which the present variance is estimated based on the new information and last estimation value with fading factors to balance the weights. Take B_1^i for example:

$$E\{B_1^i\}_0 = 0, D\{B_1^i\}_0 = 0, \tag{9a}$$

$$E\{B_1^i\}_k = \alpha_e \cdot E\{B_1^i\}_{k-1} + (1-\alpha_e) \cdot B_1^i(k), \tag{9b}$$

$$D\{B_1^i\}_k = \alpha_v \cdot D\{B_1^i\}_{k-1} + (1-\alpha_v) \cdot (B_1^i(k) - E\{B_1^i\}_k)^2, \tag{9c}$$

where

$$\alpha_e = \frac{k-1}{k}, \tag{10a}$$

$$\alpha_v = C + (1-C) \cdot \frac{D\{B_1^i\}_{k-1}}{D\{B_1^i\}_{k-1} + (B_1^i(k) - E\{B_1^i\}_{k-1})^2}, \tag{10b}$$

$$k = 1, 2, 3 \ldots \tag{10c}$$

Here $E\{\cdot\}$ stands for the average, $D\{\cdot\}$ is the variance, k denotes the epoch number, α_e and α_v are the fading factors and C $(0 < C < 1)$ is an empirical constant restricting α_v between C and 1. From the analysis above, the average of the combination is constant, so the definition of α_e is actually a classic method of averaging. However, the variance of the combination may change when the environment varies, so we have designed a new fading factor α_v to adapt possible variations. When the difference between present combination value and the average increases, α_v decreases to lower the weight of old information. C is a parameter to restrict the minimum of the fading factor, serving to avoid influence of burst noise. On the contrary, if the difference decreases, the weight of old information increases to guarantee the stability. In the extreme case, if present combination value equals the average, $\alpha_v = 1$ and the new information has no influence. The advantages of this method are that the estimation can adapt environment variation quickly and stability is guaranteed even when burst noise occurs. The variance of B_2^i can be calculated in the same way. Solving linear equation set (8), the variances of code observations can be calculated by

$$D\{\varepsilon_{P1}^i\} = \frac{(f_1+f_2)^2 \cdot D\{B_1^i\} - f_2^2 \cdot D\{B_2^i\}}{f_1^2 - f_2^2}, \tag{11a}$$

$$D\{\varepsilon_{P2}^i\} = \frac{f_1^2 \cdot D\{B_2^i\} - (f_1+f_2)^2 \cdot D\{B_1^i\}}{f_1^2 - f_2^2}. \tag{11b}$$

Taking notice of the denominator in eq. (11), extreme error propagation may occur when the two frequencies are too close. Therefore, eq. (11) is a universal expression and we assume that the error variances on two frequencies are the same if f_1 and f_2 are too close. In such a case, the code variances are calculated simply as $1/2$ of $D\{B_2^i\}$. Our simulations prove that this is an effective simple alternative. After the code variances are obtained, a rough estimation of the phase errors is sufficient for the Kalman filtering, considering that their variances are at least two orders of magnitude less than that of code observations. In Kalman filter, because the precision of phase observations is much higher than code observations, more precise estimation of the phase error variances will not change the weights significantly. Besides, too small phase error estimation value may cause too much dependence on the phase observations, so the filtering process could not resist possible residual cycle slips in practical applications. Therefore, we estimate the variances of phase errors roughly as 1/100 of the relevant code error variances. Then the variances of combination errors in eq. (3) are calculated by

$$D\{\varepsilon_1^i\}_k = \left(\frac{f_1^2}{f_1^2 - f_2^2}\right)^2 \cdot D\{\lambda_1 \varepsilon_{\Phi 1}^i\}_k + \left(\frac{f_2^2}{f_1^2 - f_2^2}\right)^2 \cdot D\{\lambda_2 \varepsilon_{\Phi 2}^i\}_k, \tag{12a}$$

$$D\{\varepsilon_2^i\}_k = \frac{1}{4} D\{\varepsilon_{P1}^i\}_k, \tag{12b}$$

$$D\{\varepsilon_3^i\}_k = \frac{1}{4} D\{\varepsilon_{P2}^i\}_k. \tag{12c}$$

Using subscript i to indicate different satellites, the covariance matrix of observation vector can be expressed simply as

$$\boldsymbol{R}_{ik} = \begin{bmatrix} D\{\varepsilon_1^i\}_k & 0 & 0 \\ 0 & D\{\varepsilon_2^i\}_k & 0 \\ 0 & 0 & D\{\varepsilon_3^i\}_k \end{bmatrix}, \tag{13}$$

$$\boldsymbol{R}_k = \begin{bmatrix} \boldsymbol{R}_{1k} & 0 & 0 \\ 0 & \ddots & 0 \\ 0 & 0 & \boldsymbol{R}_{nk} \end{bmatrix}, \tag{14}$$

where $\boldsymbol{R}_k$ is the measurement covariance matrix on epoch k in Kalman filter and n is the number of the used satellites. Without affecting filtering results, the tiny values in the covariance matrix are set to zero to simplify the calculation.

By using fading factors, the new variances can be calculated recursively, so only the results in last epoch must be preserved. In conventional RAE method, all the results in the moving window have to be preserved and new results are obtained by calculating variance again. Therefore, the new method has much lower calculation cost.

3.2 Adaptation of state covariance matrix

In Kalman filter for navigation, the state vector is set differently in static and dynamic situations. In dynamic situations, differentials of some basic state variables are needed to improve filtering precision, such as velocity and acceleration. The model is known as PVA model. Therefore, we extend eq. (6) to establish the state vector suitable to our new method under various situations. The coefficients corresponding to the added state variables in the measurement equation set are set at 0. In static situations, the state vector is defined as

$$\boldsymbol{X}_S = \begin{bmatrix} x & y & z & b & \dot{b} & N_1^1 & N_2^1 & \cdots & N_1^n & N_2^n \end{bmatrix}^{\mathrm{T}}. \tag{15}$$

Then the first-order equation in state space is established by

$$\dot{\boldsymbol{X}}_S = \boldsymbol{F}_S \cdot \boldsymbol{X}_S + \boldsymbol{w}.$$

Here system dynamics matrix $\boldsymbol{F}_S$ is a $(2n+5)$-dimension square matrix in which the fifth element in the fourth row is 1 and the others are 0. $\boldsymbol{w}$ is the process noise vector. In kinetic situations, we extend eq. (6) by the PVA model:

$$\boldsymbol{X}_D = \begin{bmatrix} \boldsymbol{U} & b & \dot{b} & \dot{\boldsymbol{U}} & \ddot{\boldsymbol{U}} & N_1^1 & N_2^1 & \cdots & N_1^n & N_2^n \end{bmatrix}^{\mathrm{T}}, \tag{16a}$$

$$\boldsymbol{U} = \begin{bmatrix} x & y & z \end{bmatrix}. \tag{16b}$$

In this situation the first-order equation in state space is established in the same form:

$$\dot{\boldsymbol{X}}_D = \boldsymbol{F}_D \cdot \boldsymbol{X}_D + \boldsymbol{w}, \tag{17a}$$

$$\boldsymbol{F}_D = \begin{bmatrix} \boldsymbol{Z} & \boldsymbol{O}^{\mathrm{T}} & \boldsymbol{O}^{\mathrm{T}} & \boldsymbol{L} & \boldsymbol{Z} & \boldsymbol{O}^{\mathrm{T}} & \cdots & \boldsymbol{O}^{\mathrm{T}} \\ \boldsymbol{O} & 0 & 1 & \boldsymbol{O} & \boldsymbol{O} & 0 & \cdots & 0 \\ \boldsymbol{O} & 0 & 0 & \boldsymbol{O} & \boldsymbol{O} & 0 & \cdots & 0 \\ \boldsymbol{Z} & \boldsymbol{O}^{\mathrm{T}} & \boldsymbol{O}^{\mathrm{T}} & \boldsymbol{Z} & \boldsymbol{L} & \boldsymbol{O}^{\mathrm{T}} & \cdots & \boldsymbol{O}^{\mathrm{T}} \\ \boldsymbol{Z} & \boldsymbol{O}^{\mathrm{T}} & \boldsymbol{O}^{\mathrm{T}} & \boldsymbol{Z} & \boldsymbol{Z} & \boldsymbol{O}^{\mathrm{T}} & \cdots & \boldsymbol{O}^{\mathrm{T}} \\ \boldsymbol{O} & 0 & 0 & \boldsymbol{O} & \boldsymbol{O} & 0 & \cdots & 0 \\ \vdots & \vdots & \vdots & \vdots & \vdots & \vdots & \ddots & \vdots \\ \boldsymbol{O} & 0 & 0 & \boldsymbol{O} & \boldsymbol{O} & 0 & \cdots & 0 \end{bmatrix}, \tag{17b}$$

$$\boldsymbol{O} = \begin{bmatrix} 0 & 0 & 0 \end{bmatrix}, \tag{17c}$$

$$\boldsymbol{Z} = \begin{bmatrix} 0 & 0 & 0 \\ 0 & 0 & 0 \\ 0 & 0 & 0 \end{bmatrix}, \boldsymbol{L} = \begin{bmatrix} 1 & 0 & 0 \\ 0 & 1 & 0 \\ 0 & 0 & 1 \end{bmatrix}, \tag{17d}$$

where $\boldsymbol{F}_D$ is a $(2n+11)$-dimension square matrix and the abridged elements are all zeros. We use $\boldsymbol{X}$ to express the state vectors in different situations and $\boldsymbol{F}$ to express the corresponding system dynamics matrix. The one-step transfer equation in discrete Kalman filter is

$$\boldsymbol{\Phi} = \boldsymbol{F} \cdot T_s + \mathbf{I}, \tag{18a}$$

$$\boldsymbol{X}_{k+1|k} = \boldsymbol{\Phi} \cdot \boldsymbol{X}_k + \boldsymbol{w}, \tag{18b}$$

where subscript k indicates the number of the epoch, T_s is the sampling interval, $\mathbf{I}$ is the unit matrix of the same dimensions, $\boldsymbol{\Phi}$ is the one-step transfer matrix and $\boldsymbol{X}_{k+1|k}$ is the one-step predicted state.

In navigation based on Kalman filter, changes of the receiver's motion usually lower the precision because of the mismatch of kinematics model and real situation. Though the usage of PVA model can relieve the mismatch, interference from higher order accelerations is still inevitable. Therefore, we make the state covariance matrix adaptive by adjusting the process-noise matrix based on the filtering results and predicted states. Compared to the methods adjusting the state covariance matrix directly, the new method can regulate the filtering process fundamentally. In practical applications, $\boldsymbol{w}$ is usually assumed to be a white noise vector, so the process-noise matrix $\boldsymbol{Q}$ is diagonal. In the new method, the differences between predicted position and filtering results are used as innovations to update matrix $\boldsymbol{Q}$ every epoch. The process can be expressed by improving classic Kalman filtering [12]:

$$\boldsymbol{D}_k = \boldsymbol{Q}_k \cdot T_s + \frac{1}{2}T_s^2(\boldsymbol{F}\boldsymbol{Q}_k + \boldsymbol{Q}_k\boldsymbol{F}^{\mathrm{T}}) + \frac{1}{3}T_s^3\boldsymbol{F}\boldsymbol{Q}_k\boldsymbol{F}^{\mathrm{T}}, \tag{19a}$$

$$\boldsymbol{P}_{k+1|k} = \boldsymbol{\Phi}\boldsymbol{P}_{k|k}\boldsymbol{\Phi}^{\mathrm{T}} + \boldsymbol{D}_k, \tag{19b}$$

$$\boldsymbol{K}_{k+1} = \boldsymbol{P}_{k+1|k}\boldsymbol{H}_{k+1}^{\mathrm{T}}(\boldsymbol{H}_{k+1}\boldsymbol{P}_{k+1|k}\boldsymbol{H}_{k+1}^{\mathrm{T}} + \boldsymbol{R}_{k+1})^{-1}, \tag{19c}$$

$$\Delta\boldsymbol{X}_{k+1} = \boldsymbol{K}_{k+1} \cdot (\boldsymbol{Y}_{k+1} - \boldsymbol{H}_{k+1} \cdot \boldsymbol{X}_{k+1|k}), \tag{19d}$$

$$\boldsymbol{Q}_{k+1} = \mathrm{diag}(\Delta\boldsymbol{X}_k^2), \tag{19e}$$

$$\boldsymbol{X}_{k+1} = \boldsymbol{X}_{k+1|k} + \Delta\boldsymbol{X}_{k+1}, \tag{19f}$$

$$\boldsymbol{P}_{k+1|k+1} = (\mathbf{I} - \boldsymbol{K}_{k+1}\boldsymbol{H}_{k+1}) \cdot \boldsymbol{P}_{k+1|k}, \tag{19g}$$

where $\boldsymbol{Q}_k$ is the process-noise matrix on epoch k, which is updated in the filtering process. $\boldsymbol{P}_{k|k}$ is the state covariance matrix. In the initial step of filtering process, $\boldsymbol{Q}_0$ is set roughly and $\boldsymbol{P}_{0|0}$ is set the same as $\boldsymbol{Q}_0$. Because $\boldsymbol{Q}_k$ is updated quickly, the initial value hardly influences the results. $\boldsymbol{R}_k$ is the measurement covariance matrix in eq. (14). $\Delta\boldsymbol{X}_k$ is the difference between predicted state and filtering result in epoch k, $\boldsymbol{K}$ is the Kalman gain, $\boldsymbol{H}_k$ is the coefficient matrix in measurement equation set established in section 2. $\boldsymbol{H}_k$ is calculated every epoch based on eq. (5) and the filtering results on last step, and diag(·) is the diagonal matrix function in MATLAB. In the process, we use $\Delta\boldsymbol{X}_k$ forming a diagonal matrix to set $\boldsymbol{Q}_{k+1}$ every epoch, which is a recursive procedure. In kinetic cases, the process can converge quickly and adapt the changes of receiver motions.

4 Simulation results

RAE method usually has higher precision than the fading filtering method. Therefore, we made comparisons between our new method and RAE method to prove its advantages based on both practical static data and kinetic simulation.

4.1 Application on practical static data

The practical data from IGS (International GNSS Service) Pigeon Point Station [13] on July 15, 2000 is chosen to prove the effectiveness of the proposed approach in static situation. The sampling time of the data is 30 s, which is set for geodesic applications. We choose the observation data from time 00:38:30 to 02:22:00 that day to practice the new and previous adaptive algorithms and make comparison. There were six visible satellites available in the period, numbered 1, 11, 16, 20, 22 and 25. In order to show the comparison results clearly, the precise ephemeris is also used to avoid extra errors. The empirical value in the new fading factor defined above is set to 0.9 and the length of moving window in RAE method is set at 10. Because the two frequencies are close, we assume that the error covariances in the two frequencies are the same, as illustrated in section 2. The filtering results of different methods in ECEF coordinate system are shown in the following figures, in which the vertical coordinates show the positioning error and horizontal coordinates are epochs. Positioning errors corresponding to the RAE method and the improved method proposed in this paper are compared in Figure 1. The three plots correspond to the three axes in ECEF coordinate system, and the initial position is obtained by least squares method.

From the results shown in Figure 1, we can see that the two methods are both effective. In detail, the new approach has less error than the RAE method, especially in the incipient several epochs. Gradual biases exist between filtering results and the true position because the observations are affected by residuals after tropospheric refraction correction. Because the observation environment changes slowly and the receiver is motionless, the improved adaptation of covariance matrix cannot show its advantages signally. The results show that the proposed approach in this paper can be applied to static positioning effectively.

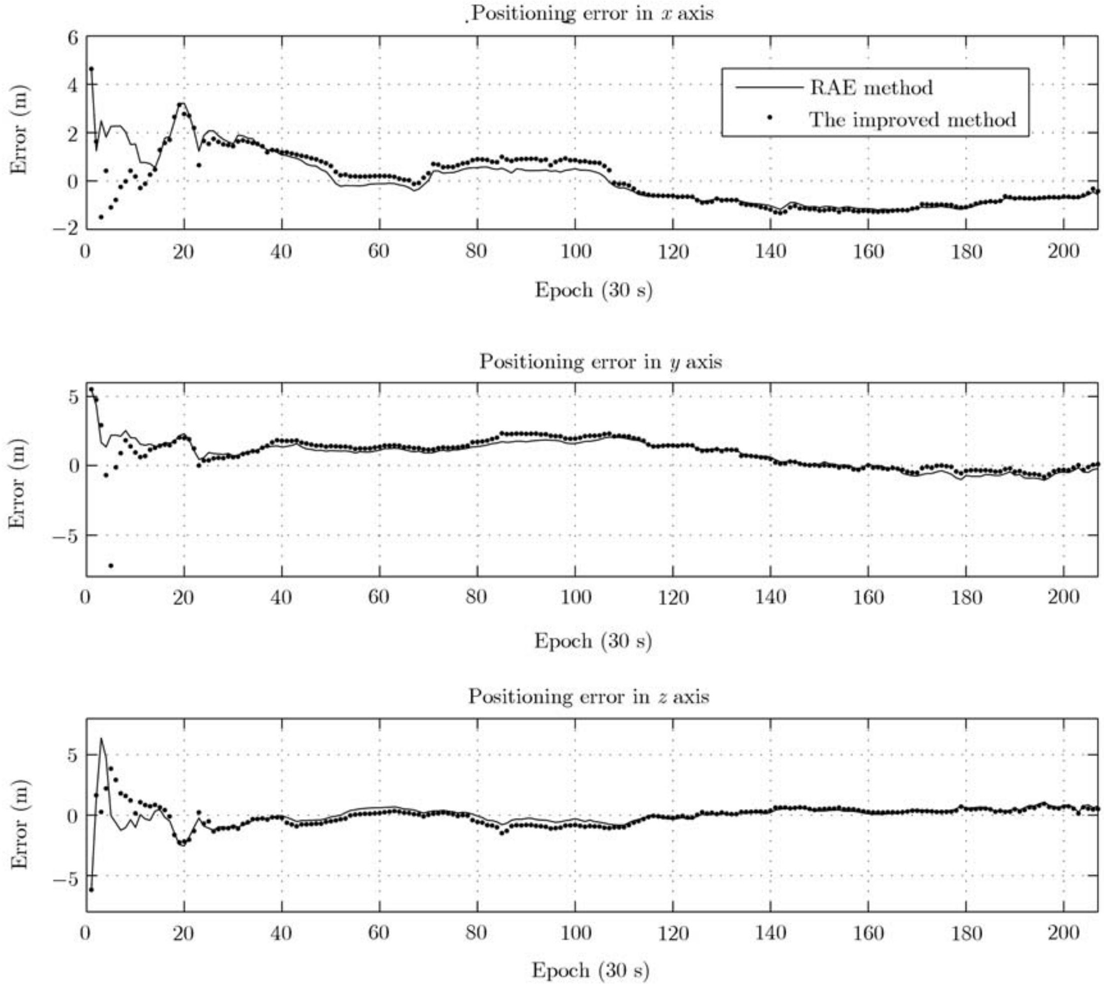

Figure 1 Positioning errors of RAE method and the improved method on static data.

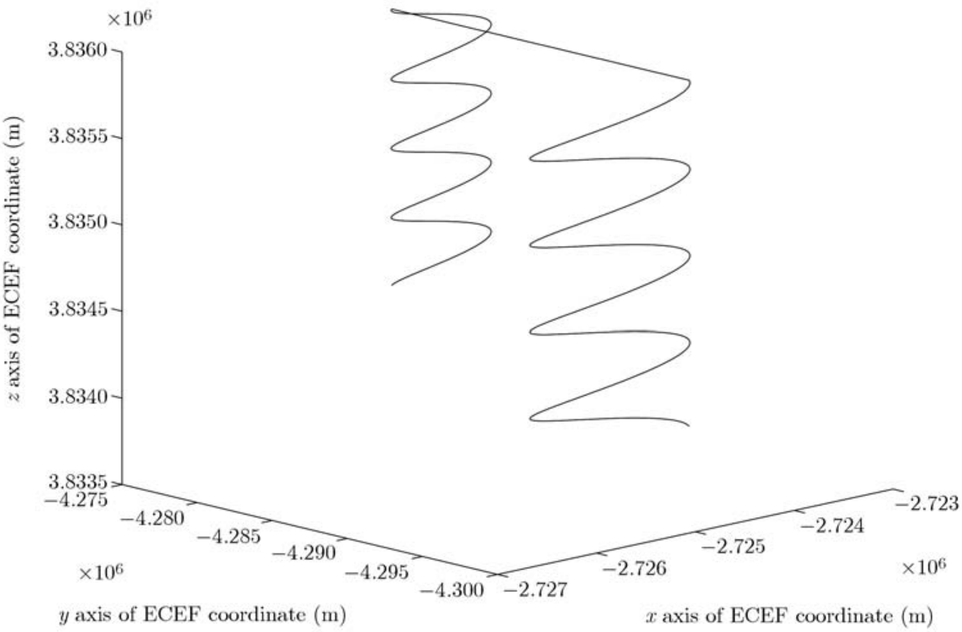

Figure 2 Simulated receiver's motion locus in ECEF coordinate system.

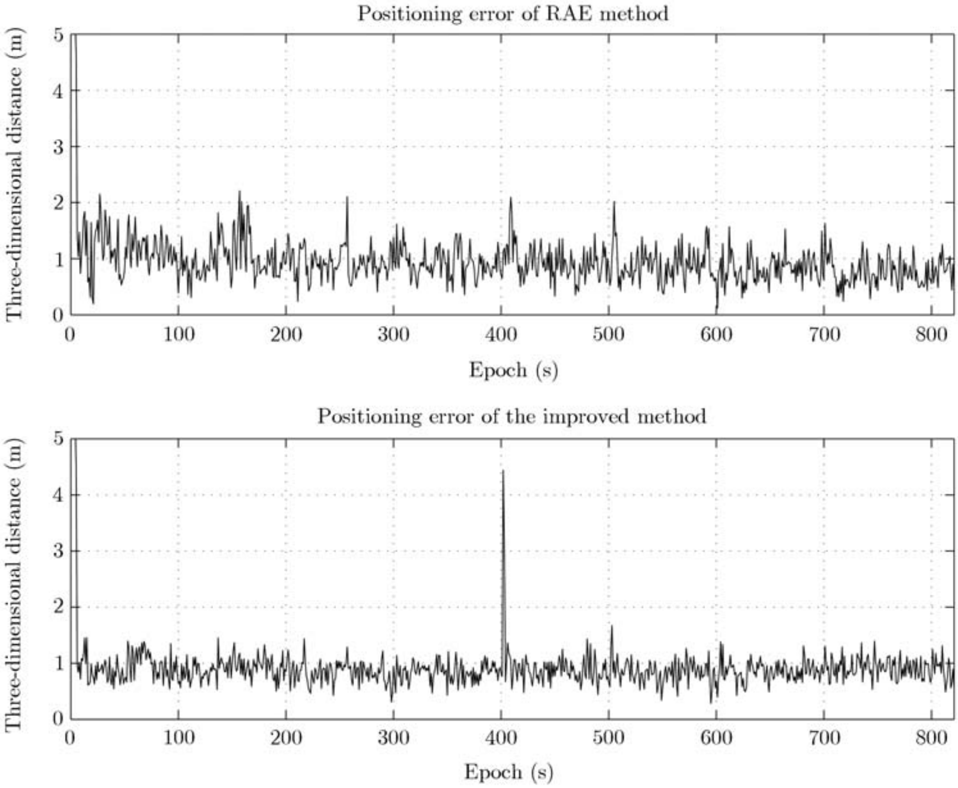

Figure 3 Comparison between the RAE method and the improved method under noise of 2 m standard deviation.

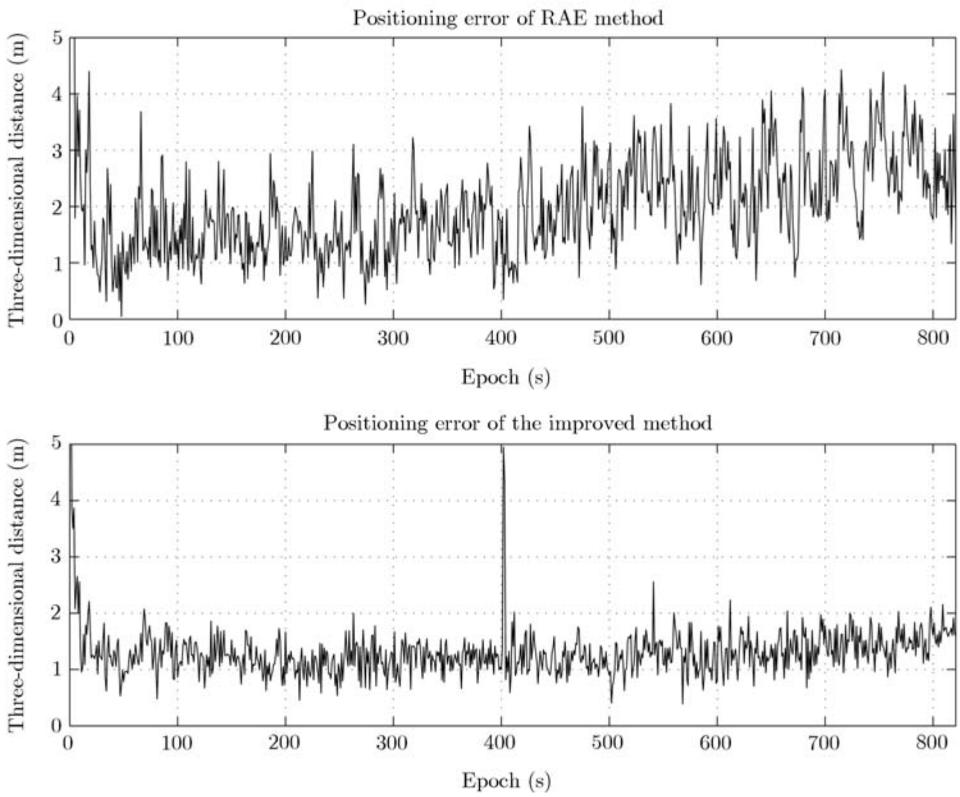

Figure 4 Comparison between the RAE method and the improved method under noise of 3 m standard deviation.

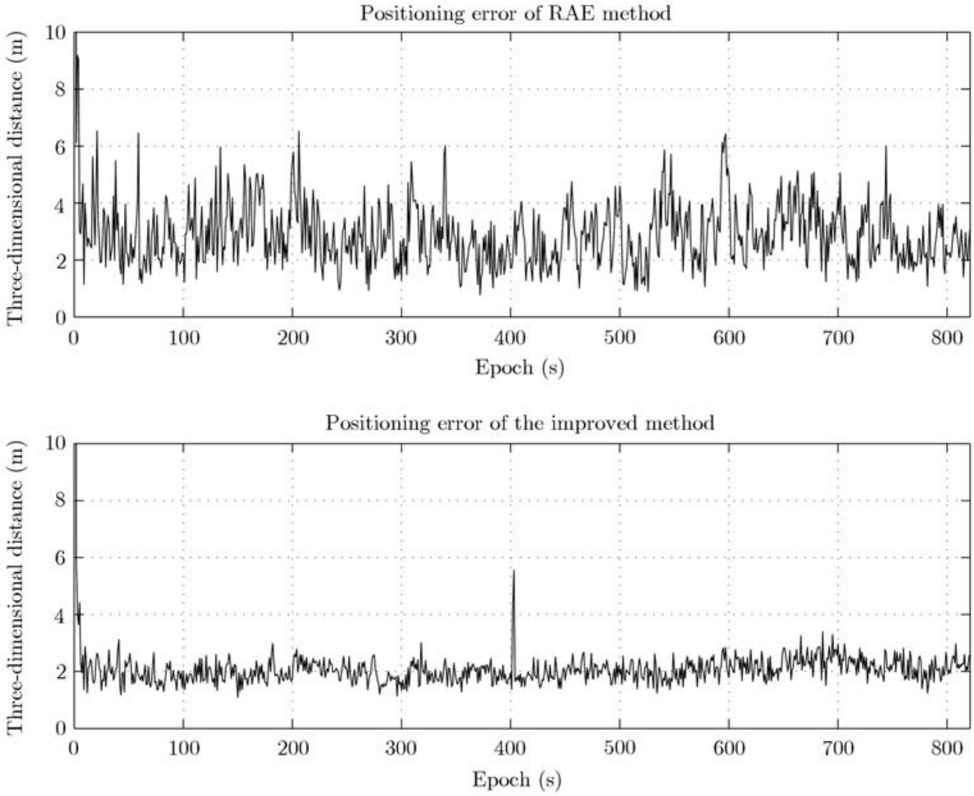

Figure 5 Comparison between the RAE method and the improved method under noise of 4 m standard deviation.

4.2 Kinetic simulation

In order to prove the advantages of the new algorithm in kinetic applications, we simulate kinetic situation based on the practical data above. Around the position of Pigeon Point Station, the receiver's motion locus is designed in ECEF coordinate system as shown in Figure 2. There are three parts in the locus: In the first spiral line part, the radius is 800 m, velocity is 51 m/s, acceleration is about 3.2 m/s^2; in the straight line part, the velocity is 200 m/s, acceleration is 0; and in the second spiral line part, the radius is 500 m, velocity is 40 m/s, acceleration is about 2.9 m/s^2. The spiral locus makes the receiver have more high-order accelerations, which is challenging for the navigation filtering. In order to compare the two methods in different observation environments, we add white noises with standard deviations of 2, 3 and 4 m to the code observations separately. Since the phase observations are much more precise than the code observations, they are hardly affected by the environments. We add white noise with a standard deviation of 5 cm in phase observations. Because the ionosphere influence is eliminated in the observation equation, it is not involved in the simulation. In order to accord with the practical kinetic application, the sampling interval in the simulation is 1 s.

The parameters of RAE method and the improved method are set the same as in practical application above. Applying RAE method and the improved method to these situations of different noise levels, comparisons are shown in Figures 3–5. We calculated the three-dimensional distances between filtering results and simulated positions to measure positioning errors on the three coordinate axes.

Comparing the results of the RAE method and the improved method, we can see that the new approach proposed in this paper is more stable and more precise. Because the receiver's kinetic motion changes (on epoch 401 and epoch 501), the RAE method cannot adapt well and the positioning results jitter more sharply, especially when the noise level is higher. By using the improved method, though a bias may happen on the epoch when the receiver's motion changes extremely, as shown on epoch 401, the filtering process can adapt in about 3 epochs. After the adaptation process, a precision higher than that of the RAE method is regained. The results of the simulation show that the new approach is superior to previous method in kinetic situations.

5 Conclusions

In this paper an improved adaptive Kalman filter for navigation using carrier phase is developed. By updating state covariance matrix and measurement covariance matrix separately every epoch, the filter can adapt the motion of receiver in various environments. Furthermore, a more effective fading factor is also proposed to make the estimation stable and adaptive. Applicable to both practical static data and kinetic simulation, the new adaptive filter proves more effective than previous adaptive methods especially in kinetic situations.

References

1 Zhang Z T, Zhang J S. A novel strong tracking finite-difference extended Kalman filter for nonlinear eye tracking. Sci China Ser F-Inf Sci, 2009, 52: 688–694
2 Yang Y X, Gao W G. Comparison of adaptive factors in Kalman filters on navigation results. J Navigation, 2005, 58: 471–478
3 Mohamed A H, Schwarz K P. Adaptive Kalman filtering for INS/GPS. J Geodesy, 1999, 73: 193–203
4 Bian H W, Jin Z H, Wang J P. The innovation-based estimation adaptive Kalman filter algorithm for INS/GPS integrated navigation system. J Shanghai Jiaotong Univ, 2006, 40: 1000–1009
5 Sinha A, Kirubarajan T, Bar-Shalom Y. Application of the Kalman-Levy filter for tracking maneuvering targets. IEEE Trans Aerospace Electron Syst, 2007, 43: 1099–11077
6 Han B, Lin X G. Adapt the steady-state Kalman gain using the normalized autocorrelation of innovations. IEEE Signal Proc Let, 2005, 12: 780–783
7 Sarkka S, Nummenmma A. Recursive noise adaptive Kalman filtering by variational Bayesian approximations. IEEE Trans Automat Contr, 2009, 54: 596–600
8 Wang J Z, Milstein L B. CDMA overlay situations for microcellular mobile communications. IEEE Trans Commun, 1995, 43: 603–614
9 Khanafseh S, Pervan B. New approach for calculating position domain integrity risk for cycle resolution in carrier phase navigation systems. IEEE Trans Aerospace Electron Syst, 2010, 46: 296–307
10 Hao M, Wang Q L, Cui D X. Study on fast convergence method in precise point positioning. J Geodesy and Geodyn, 2009, 29: 88–99
11 Wu J F, Huang C. GPS precise point positioning models and their utility models. J Geodesy Geodyn, 2008, 28: 96–100
12 Lu Y. GPS Global Positioning Receiver—Principles and Software Realization. Beijing: Publishing House of Electronics Industry, 2009
13 John M, Dow J M, Neilan R E, et al. The international GNSS service in a changing landscape of global navigation satellite systems. J Geodesy, 2009, 83: 191–198